SELF-PRESERVATION OF THE TRANSPORT EQUATIONS IN A FREE ROUND TURBULENT JET

Hamed Sadeghi and Philippe Lavoie
Institute for Aerospace Studies, University of Toronto, Toronto, M3H 5T6, Canada
sadeghi@utias.utoronto.ca, lavoie@utias.utoronto.ca

Andrew Pollard
Department of Mechanical and Materials Engineering, Queen's University, Kingston, ON, K7L 3N6, Canada
pollarda@queensu.ca

ABSTRACT

A similarity analysis is applied to the transport equations for the second-order velocity structure functions of $\langle(\delta u)^2\rangle$ and $\langle(\delta q)^2\rangle$ along the centreline of a round turbulent jet. On the basis of the current analysis, self-similar forms of the transport equations are obtained. These self-similar equations have the desirable benefit to require less extensive measurements to calculate the inhomogeneous terms of the transport equations. The validity of these equations is investigated via hot-wire measurements of velocity fluctuations. The present similarity form of the transport equation for $\langle(\delta q)^2\rangle$ is shown to be closely satisfied by the experimental data, while the assumption of isotropy leads to a significant imbalance in the equation for $\langle(\delta u)^2\rangle$. The current analysis argues that the similarity assumptions in combination with the linear decay of the mean velocity are enough to predict a power-law decay of turbulent kinetic energy, $\langle q^2\rangle$, as well as turbulent velocity fluctuations ($\langle u^2\rangle$ and $\langle v^2\rangle$). The theoretical solutions are tested against new experimental data obtained along the centreline of a round turbulent jet at $Re_D = 50,000$.

INTRODUCTION

Kolmogorov (1941) derived an important exact relation between the second- and third-order moments of the longitudinal velocity increment from the Navier-Stokes equations assuming homogeneity, isotropy (HIT) and sufficiently high Reynolds number conditions, viz.

$$-\langle(\delta u)^3\rangle + 6\nu\frac{\mathrm{d}}{\mathrm{d}r}\langle(\delta u)^2\rangle = \frac{4}{5}\langle\varepsilon\rangle r\,, \quad (1)$$

where $\delta u = u(x+r) - u(x)$, and r is the separation between the longitudinal direction x, ν is the kinematic viscosity and $\langle\varepsilon\rangle$ is the mean dissipation rate of turbulent kinetic energy. This equation implies that at a scale r the dissipation of turbulent kinetic energy is the sum of turbulent advection (first term left-hand side in (1)) and molecular diffusion (second term left-hand side in (1)).

However, the assumption that the Reynolds number should be very large is not realized in turbulent flows encountered in laboratory conditions such as gird turbulence, fully developed channel and jets. Therefore, (1) cannot be balanced for these practical flows. As such, Danaila *et al.* (1999) revisited the hypotheses involved in the derivation of (1) and derived a new equation for decaying turbulence as:

$$-\langle(\delta u)^3\rangle + 6\nu\frac{\mathrm{d}}{\mathrm{d}r}\langle(\delta u)^2\rangle - \frac{3U}{r^4}\int_0^r s^4\frac{\partial}{\partial x}\langle(\delta u)^2\rangle\mathrm{d}s = \frac{4}{5}\langle\varepsilon\rangle r. \quad (2)$$

Here, U is the mean streamwise velocity, and x is the downstream location and s is a dummy separation variable. The third term on the LHS of (2) reflects the inhomogeneity due to the streamwise decay of $\langle u^2\rangle$, which was introduced as a consequence of low Re condition. The terms in this equation can be measured by using a single hot-wire. Assuming the global isotropy, this equation can be also applied along a round jet centreline.

Later, Danaila *et al.* (2004) derived a scale-by-scale energy equation along the centreline of a turbulent round jet using the same procedure used in Danaila *et al.* (1999) and Danaila *et al.* (2002), viz.

$$-\langle(\delta u)(\delta q)^2\rangle + 2\nu\frac{\mathrm{d}}{\mathrm{d}r}\langle(\delta q)^2\rangle - \frac{U}{r^2}\int_0^r s^2\frac{\partial}{\partial x}\langle(\delta q)^2\rangle\mathrm{d}s$$
$$-2\frac{\partial U}{\partial x}\frac{1}{r^2}\int_0^r s^2(\langle(\delta u)^2\rangle - \langle(\delta v)^2\rangle)\mathrm{d}s = \frac{4}{3}\langle\varepsilon\rangle r\,. \quad (3)$$

Here, $\langle(\delta q)^2\rangle$ $(= \langle(\delta u)^2\rangle + \langle(\delta v)^2\rangle + \langle(\delta w)^2\rangle)$ is the total turbulent energy structure function. This equation has one extra term than (2), which is related to the energy production. Equation (3) is more general than (2) and only requires a local isotropy assumption, whereas (2) was derived with the use of global isotopy. Terms in (3) can be measured experimentally using a cross-wire.

In order to compute the inhomogeneous decay terms in (2) and (3), $\langle(\delta u)^2\rangle$ and $\langle(\delta q)^2\rangle$ have to be measured at different streamwise locations, which involves significant uncertainties associated with the numerical differentiation of the data Antonia & Burattini (2006). Therefore, the main goal of the current work is to apply a novel similarity analysis and introduce self-similar forms to (2) and (3). If global isotropy is assumed along the jet centreline, the production term is zero; therefore, (2), which has been previously obtained for grid turbulence, can be applied along the centreline. A particularly useful feature of this analysis is that it reduces some of the difficulties involved in the calculation of the $\partial/\partial x$ terms (production and decay terms). Based on our analysis, the similarity variables are formally obtained from the governing equations. In addition, the current work assess the degree that similarity is satisfied with and without relaxing the isotropy requirement. The similarity solutions obtained are then tested against experimental measurements taken along the centreline of a round jet.

THEORETICAL CONSIDERATION

The concept of similarity, or self-preservation, which assumes the flow scales with single velocity and length scales, has been an important analytical tool in turbulence research. In this work, an equilibrium similarity analysis, first introduced by George (1992), is developed for the transport equation of the second-order energy structure function of $\langle(\delta q)^2\rangle$ along the centreline of a round turbulent jet (3). The equilibrium similarity forms of the second- and third-order structure functions of u, v and q are required to obtain the similarity form of (3). Following the same procedure as George (1992), Danaila *et al.* (2004) and Sadeghi *et al.* (2015), we can show that these are given by

$$f(r/\lambda) = \langle(\delta q)^2\rangle/\langle q^2\rangle, \tag{4}$$

$$e(r/\lambda) = \langle(\delta u)^2\rangle/\langle u^2\rangle, \tag{5}$$

$$h(r/\lambda) = \langle(\delta v)^2\rangle/\langle v^2\rangle \tag{6}$$

and

$$g(r/\lambda) = -\langle(\delta u)(\delta q)^2\rangle/(3^{-1/2}Re_\lambda^{-1}\langle q^2\rangle^{3/2}). \tag{7}$$

respectively. Here, g is the normalized third-order structure function, and f, e and h are the normalized second-order structure functions. Assuming axisymmetry, $\langle q^2\rangle = \langle u^2\rangle + 2\langle v^2\rangle$. The accuracy of this assumption has been confirmed both on and off the centreline of round jets by Hussein *et al.* (1994). The general definitions of Taylor microscale and Taylor microscale Reynolds number are:

$$\lambda^2 = 5\nu\frac{\langle q^2\rangle}{\langle\varepsilon\rangle}, \tag{8}$$

and

$$Re_\lambda = \frac{\langle q^2\rangle^{1/2}\lambda}{3^{1/2}\,\nu}. \tag{9}$$

respectively, (Antonia *et al.*, 2003; Burattini *et al.*, 2005*b*). One possible equilibrium similarity solution of (3) is a power-law of the form

$$\langle q^2\rangle = A(x-x_0)^m, \tag{10}$$

where x_0 is the virtual origin, m is the power-law exponent and A is a constant of proportionality. The same power-law behaviour is also suggested for $\langle u^2\rangle$ and $\langle v^2\rangle$ as

$$\langle u^2\rangle = A_1(x-x_0)^m \tag{11}$$

and

$$\langle v^2\rangle = A_2(x-x_0)^m. \tag{12}$$

The virtual origin follows from the variation of the mean velocity along the centreline, viz.

$$U = C/(x-x_0), \tag{13}$$

where C is a constant. For the region near the axisymmetric jet centreline, Burattini *et al.* (2005*a*) approximated the kinetic energy budget equation as

$$\langle\varepsilon\rangle_{ls,q} = -\frac{U}{2}\frac{\mathrm{d}\langle q^2\rangle}{\mathrm{d}x} - (\langle u^2\rangle - \langle v^2\rangle)\frac{\mathrm{d}U}{\mathrm{d}x}. \tag{14}$$

The subscript "ls,q" indicates that the dissipation is evaluated from the large-scale quantities via the energy budget of $\langle q^2\rangle$. Assuming axisymmetry, introducing (10)-(13) into (14), we obtain

$$\langle\varepsilon\rangle_{ls,q} = C\left[\frac{-(A_1+2A_2)m}{2} + (A_1-A_2)\right](x-x_0)^{m-2}. \tag{15}$$

The similarity form of (3) follows after substituting (4)-(7) and (15) into (3), viz.

$$g + 2\frac{\mathrm{d}f}{\mathrm{d}(r/\lambda)} + 10(c_1+2c_2)\frac{\Gamma_1}{(r/\lambda)^2} - 10m(c_1+2c_2)\frac{\Gamma_2}{(r/\lambda)^2} + 20c_1\frac{\Gamma_3}{(r/\lambda)^2} - 20c_2\frac{\Gamma_4}{(r/\lambda)^2} = \frac{20}{3}(r/\lambda), \tag{16}$$

where Γ_1, Γ_2, Γ_3 and Γ_4 are given by

$$\Gamma_1 = \int_0^{r/\lambda}\left(\frac{s}{\lambda}\right)^3\frac{\mathrm{d}f}{\mathrm{d}(r/\lambda)}\mathrm{d}\left(\frac{s}{\lambda}\right), \quad \Gamma_2 = \int_0^{r/\lambda}\left(\frac{s}{\lambda}\right)^2 f\,\mathrm{d}\left(\frac{s}{\lambda}\right),$$

$$\Gamma_3 = \int_0^{r/\lambda}\left(\frac{s}{\lambda}\right)^2 e\,\mathrm{d}\left(\frac{s}{\lambda}\right), \quad \Gamma_4 = \int_0^{r/\lambda}\left(\frac{s}{\lambda}\right)^2 h\,\mathrm{d}\left(\frac{s}{\lambda}\right).$$

Here,

$$c_1 = \frac{A_1}{-Am+2(A_1-A_2)} \tag{17}$$

and

$$c_2 = \frac{A_2}{-Am+2(A_1-A_2)}. \tag{18}$$

Dividing by $(20/3)r/\lambda$, (16) can be rewritten symbolistically as

$$A^* + B^* + D^* + P^* = C^*. \tag{19}$$

where A^* is the turbulent advection term (the first term in (16)), B^* is the diffusion term (the second term in (16)), D^* is the inhomogeneous decay term along streamwise direction x (the sum of third and forth terms in (16)), P^* is the production term (the sum of fifth and sixth terms in (16)) and C^* is the balance of all other terms.

The assumption of isotropy has been extensively used in the literature to estimate dissipation and some other characteristics of jet flows. In this case, only one component of the flow (u) is measured using a single-wire. The equilibrium similarity expression of $\langle(\delta u)^2\rangle$ and $\langle(\delta u)^3\rangle$ are required to obtain the similarity form of (2). Using the same procedure as Sadeghi *et al.* (2015), we can show that these are given by

$$f_u(r/\lambda_u) = \langle(\delta u)^2\rangle / \langle u^2\rangle, \tag{20}$$

and

$$g_u(r/\lambda_u) = -\langle(\delta u)^3\rangle / (Re_{\lambda_u}^{-1} \langle u^2\rangle^{3/2}), \tag{21}$$

where the subscript u is used to identify quantities related to the transport equation of $\langle(\delta u)^2\rangle$.

The isotropic definitions of the Taylor microscale and Taylor microscale Reynolds number, which are the appropriate parameters for the transport equation of $\langle(\delta u)^2\rangle$, are defined as

$$\lambda_u^2 = 15\nu \frac{\langle u^2\rangle}{\langle\varepsilon\rangle}, \tag{22}$$

and

$$Re_{\lambda_u} = \frac{\langle u^2\rangle^{1/2}\lambda_u}{\nu}. \tag{23}$$

The dissipation can be obtained from the isotropic form of the mean energy budget, viz.

$$\langle\varepsilon\rangle_{ls,u} = \frac{-3U}{2}\frac{\mathrm{d}\langle u^2\rangle}{\mathrm{d}x}. \tag{24}$$

Equation (24) is used to remain consistent with the isotropic assumption that was used to derive equation (2). Substitution of (20), (21) and (24) into (2) yields a similarity from of (2), viz.

$$g_u + 6\frac{\mathrm{d}f_u}{\mathrm{d}(r/\lambda_u)} + \frac{30}{m}\frac{\Gamma_{u1}}{(r/\lambda_u)^4} - 30\frac{\Gamma_{u2}}{(r/\lambda_u)^4} = 12(r/\lambda_u). \tag{25}$$

where Γ_{u1} and Γ_{u2} are given by

$$\Gamma_{u1} = \int_0^{r/\lambda_u}\left(\frac{s}{\lambda_u}\right)^5 \frac{\mathrm{d}f_u}{\mathrm{d}(r/\lambda_u)}\,\mathrm{d}\left(\frac{s}{\lambda_u}\right),$$

$$\Gamma_{u2} = \int_0^{r/\lambda_u}\left(\frac{s}{\lambda_u}\right)^4 f_u\,\mathrm{d}\left(\frac{s}{\lambda_u}\right).$$

Dividing by $12(r/\lambda_{iso})$, (25) can be rewritten as

$$A_u^* + B_u^* + D_u^* = C_u^*. \tag{26}$$

Experimental details

Experimental measurements were performed to test the similarity solutions obtained in the previous section. An air jet was generated using a fan mounted on anti-vibration pads. The air then exits a settling chamber via a round duct to the inlet of a smoothly contracting axisymmetric nozzle. The experiments were carried out at the exit Reynolds number of $Re_D = 50,000$, where Re_D is calculated based on the jet exit mean velocity ($U_j = 10.65$ m/s) and the nozzle exit diameter $D = 0.0736$ m. The jet has a top-hat velocity profile at the exit. The axial turbulence intensity in the potential core of the flow near the jet exit was less than 0.7% (see Sadeghi & Pollard (2012); Sadeghi *et al.* (2014) for further details about the exit conditions of the jet). The measurements were performed for $10 \leq x/D \leq 20$. Measurements of the turbulence statistics were obtained using both singe and cross-wire probes. The wires were made of 2.5 micron diameter tungsten wire with a 0.5 mm sensing length. The hot-wires were calibrated in the jet core before and after each experiment. Similar to the scheme described in Burattini & Antonia (2005), the cross-wire was calibrated using a look-up table, with calibration angles within the range ± 40, in intervals of 10°. The signals were low-pass filtered at a cut-off frequency f_c, which was selected based on the onset of electronic noise and close to the Kolmogorov frequency, $f_k \equiv U/2\pi\eta$, where η is Kolmogorov length scale. The measurements were taken with a sampling frequency of $f_s \geq 2f_c$. The sampling time was selected to ensure enough data were taken to achieve statistical convergence of $\langle q^2\rangle$ (at least within $\pm 2\%$) and in the peak value of the generalised normalised third-order structure function $\langle(\delta u)^2(\delta q)\rangle$ (at least within $\pm 4\%$, which typically required 10 min. sampling time). In the present work, the modified Taylor hypothesis based on the models developed by Lumley (1965) was used to convert time into a spatial series. In addition, data were corrected for the effect of high frequency noise and finite spatial resolution (Hearst *et al.*, 2012; Xu *et al.*, 2013; Sadeghi *et al.*, 2014). A few basic quantities measured at three selected axial locations are summarized in Table 1 for reference. Here, $\langle\varepsilon\rangle_{\mathrm{iso}}$ is an estimation for dissipation based on the local isotropy assumption, viz.

$$\langle\varepsilon\rangle_{iso} = 15\nu\left\langle\left(\frac{\partial u}{\partial x}\right)^2\right\rangle, \tag{27}$$

while $\langle\varepsilon\rangle_{\mathrm{hom}}$ is obtained by only the much less restrictive assumptions of homogeneity and axisymmetirc using a cross-wire, viz.

$$\langle\varepsilon\rangle_{hom} = 3\nu\left[\left\langle\left(\frac{\partial u}{\partial x}\right)^2\right\rangle + 2\left\langle\left(\frac{\partial v}{\partial x}\right)^2\right\rangle\right]. \tag{28}$$

In Table 1, λ_{hom} and λ_{iso} are calculated by replacing $\langle\varepsilon\rangle_{\mathrm{hom}}$ and $\langle\varepsilon\rangle_{\mathrm{iso}}$ into (8) and (22), respectively. $Re_{\lambda_{\mathrm{hom}}}$ is obtained

x/D	$\langle\varepsilon\rangle_{\text{hom}}$ (m^2s^{-3})	$\langle\varepsilon\rangle_{\text{iso}}$ (m^2s^{-3})	λ_{hom} (mm)	λ_{iso} (mm)	$Re_{\lambda_{\text{hom}}}$	$Re_{\lambda_{\text{iso}}}$	η_{hom} (mm)	η_{iso} (mm)
10	33.9	37	3.16	3.45	242	302	0.103	0.101
15	9.30	13	4.36	4.21	242	265	0.143	0.131
20	3.40	5.63	5.64	4.98	243	245	0.219	0.189

Table 1: A few basic parameters at three downstream locations along the jet centreline of the jet.

from (9) using λ_{hom} while $Re_{\lambda_{\text{iso}}}$ is calculated from (23) using λ_{iso}. The Kolmogorov length scales of η_{hom} and η_{iso} are obtained by replacing $\langle\varepsilon\rangle_{\text{hom}}$ and $\langle\varepsilon\rangle_{\text{iso}}$ into

$$\eta \equiv \nu^{3/4}/\langle\varepsilon\rangle^{1/4}. \tag{29}$$

EXPERIMENTAL RESULTS

The axial mean velocity along the jet centreline is presented in Figure 1. As expected, it decays linearly with axial distance. For a self-similar jet, the centreline velocity variation can be written as

$$\frac{U_j}{U_c} = \frac{1}{B}\left(\frac{x-x_0}{D}\right), \tag{30}$$

which is the inverted normalised form of (13). A least-squares fit to the data gives a mean velocity decay constant of $B = 6.6$ (or $C = B*D*U_j = 5.17$) and a virtual origin of $x_0 = -1.69D$. Here, B is very similar to the values obtained by Weisgraber & Liepman (1998) and Ferdman *et al.* (2000) ($B \sim 6.7$) and in good agreement with Panchapakesan & Lumley (1993) and Burattini *et al.* (2005*b*) ($B \sim 6.1$). It is generally accepted that there is some variability in the mean velocity decay constant and virtual origin (e.g., see Table 1 in Fellouah *et al.*, 2009) for different experiments, which has typically been related to differences in the measurement region, exit Reynolds number, experimental technique used and initial conditions (Xu & Antonia, 2002).

The streamwise variations of $\langle q^2\rangle$, $\langle u^2\rangle$ and $\langle v^2\rangle$, measured along the jet centreline and normalised by U_j^2, are shown in Figure 2. A curve fit was applied to the data using the virtual origin of $x_0 = -1.69D$. It was found that $\langle q^2\rangle$, $\langle u^2\rangle$ and $\langle v^2\rangle$ follow closely a power-law with exponent $m = -1.83$, in agreement with (10-12). The decay rate constants for $\langle q^2\rangle$, $\langle u^2\rangle$ and $\langle v^2\rangle$ are estimated to be $A = 3.29$, $A_1 = 1.43$ and $A_2 = 0.93$, respectively.

In order to further confirm the analytical solutions with the experimental results, distributions of $f(r/\lambda_{\text{hom}})$ measured at the three locations considered here ($x/D = 10$, 15 and 20) are shown in Figure 3. The second-order structure functions of q are found to collapse approximately at each streamwise location, which suggest that the similarity parameters found in the analysis are justified. The distributions of $e(r/\lambda_{\text{hom}})$ and $h(r/\lambda_{\text{hom}})$ are also shown in Figure 3. The second-order structure functions of u and v are also found to collapse approximately using the normalization parameters.

Attention is now turned to (16) and (25), which have been derived as the similarity forms of (3) and (2), respectively. First, in order to illustrate the validity of (16), the

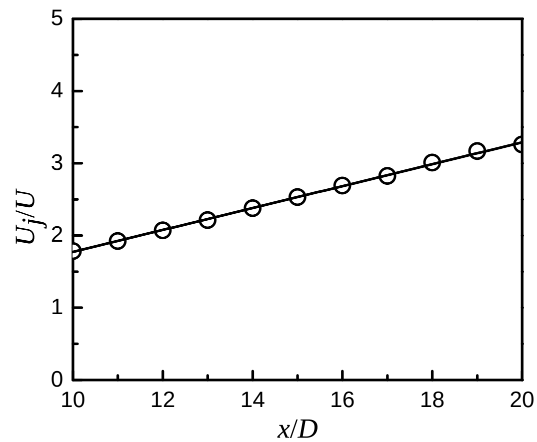

Figure 1: Axial decay of the mean velocity along the centreline. Solid line is the least squares fit to the data.

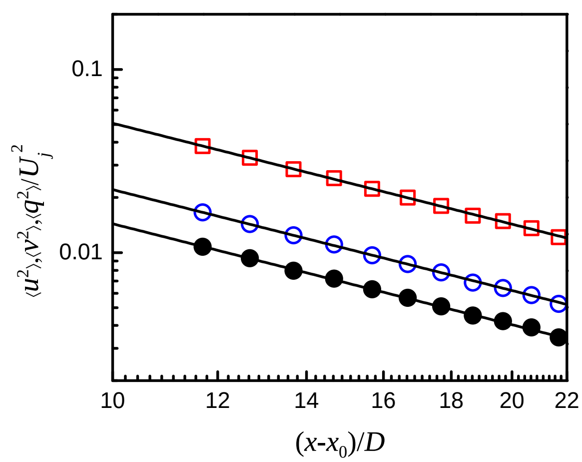

Figure 2: Streamwise variation of $\langle q^2\rangle$ (□), $\langle u^2\rangle$ (○) and $\langle v^2\rangle$ (●) along the centreline.

term $g(r/\lambda_{\text{hom}})$ is calculated from equation (16) using the corresponding power-law exponent m and the decay rates A_1 and A_2 at $x/D = 15$ (identified as g_c) and compared with the measured profile of $g(r/\lambda_{\text{hom}})$ (denoted by g_m) in Figure 4. A relatively good agreement (within $\pm 11\%$) is found between g_m and g_c. The third-order structure functions are normalised using r/λ_{hom} so that their maximum peaks can be compared with the onset of the inertial range. It can be observed that the asymptotic value of 20/3, which rep-

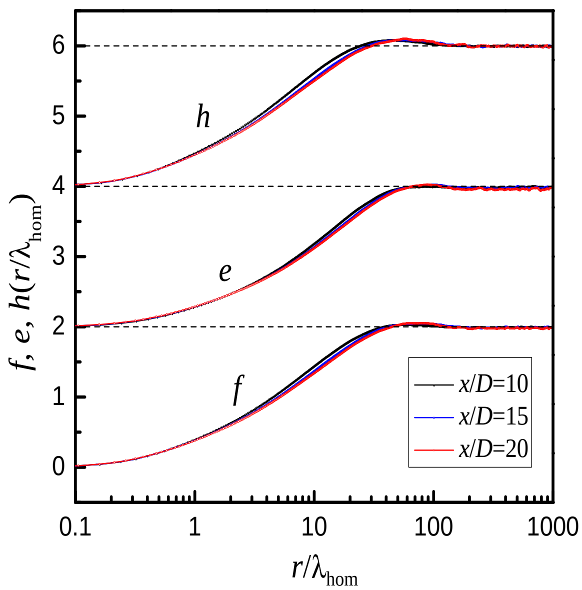

Figure 3: Distributions of $f, e, h(r/\lambda_{\text{hom}})$ at three axial locations of $x/D = 10, 15, 20$. Structure functions have been shifted successively (offset 2) with respect to the lower one. Each horizontal dashed line is 2.

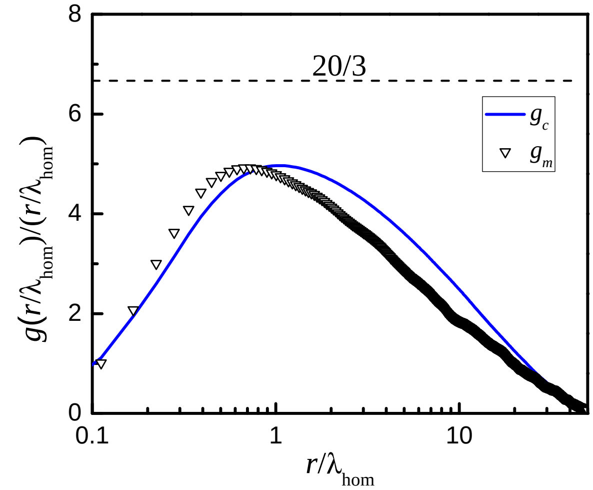

Figure 4: Comparison between measured (triangles) and calculated (from eqn. 16, solid line) distributions of g divided by r/λ_{hom}(at $x/D = 15$).

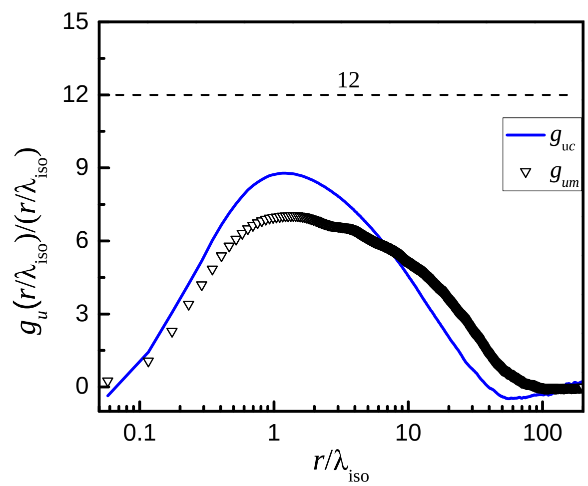

Figure 5: Comparison between measured (triangles) and calculated (from eqn. 25, solid line) distributions of g_u divided by r/λ_{iso}(at $x/D = 15$). Dashed line is 12.

resents the onset of the inertial range for a high Reynolds number, is significantly higher than the maximum measured and calculated g. Sadeghi *et al.* (2014) showed that a proper inertial range is unlikely to be established along the jet axis unless a very high Reynolds number of $Re_\lambda = 10^4$ can be reached.

In order to study the accuracy of (25), the term $g_u(r/\lambda_{\text{iso}})$, which is calculated from (25) (identified as g_{uc}), is compared with the measured profile of $g_u(r/\lambda_{\text{iso}})$ (denoted by g_{um}) in Figure 5 at $x/D = 15$. The same trend in profiles g_{uc} and g_{um} confirms somewhat the analysis used to derive(25). However, a larger difference (within $\pm 25\%$) between the measured and calculated normalized third-order structure functions can be observed when (25) is used. This suggests that the assumptions used to obtain (25), while only one component of the flow is measured by using a single-wire, are less accurate than those applied in (16). It is then concluded that (16) is more appropriate for studying the scale-by-scale budget for jet flows in the region where similarity is satisfied to a good approximation.

The scale-by-scale budget terms in (19), which is a normalised form of (16), measured at $x/D = 15$ in terms of r/λ_{hom} are given in Figure 6. This figure demonstrates that (16) is adequately satisfied by the experimental data over nearly all scales (i.e., $A^* + B^* + D^* + P^* \approx C^*$). At small r/λ_{hom}, the diffusion term B dominates, while at large r/λ_{hom}, the decay term D^* and the production term P^* are the dominant terms. A very good balance of all terms at very large scales confirms the similarity forms of the production P^* and inhomogeneous decay D^* terms. The advection term A^* goes to zero at both small and large separations, while its maximum is located around $r \simeq 0.8\lambda_{\text{hom}}$, which is similar to previous observations from grid turbulence experiments and along a jet centreline (Burattini *et al.*, 2005*a*). The peak value of the advection term A^* occurs at a value of r/λ_{hom} in the vicinity of $B^* = D^*$. The production term P^* becomes important around $r/\lambda_{\text{hom}} \gtrsim 8$, where the value of the diffusion term B^* begins to decrease at a higher rate with increasing r/λ_{hom}. This point is very close to the value of r/λ_{hom} where $A^* = D^*$.

CONCLUSION AND ONGOING WORK

Using an equilibrium similarity analysis, the similarity forms of the transport equations of the second-order velocity structure functions of $\langle(\delta q)^2\rangle$ and $\langle(\delta u)^2\rangle$ were obtained along the centreline of a turbulent round jet. The important consequence of the current analysis was to obtain the forms for the decay law directly from the governing equations. It was shown that the self-similar analysis of the equations yield to a solution where the turbulent kinetic energy decays

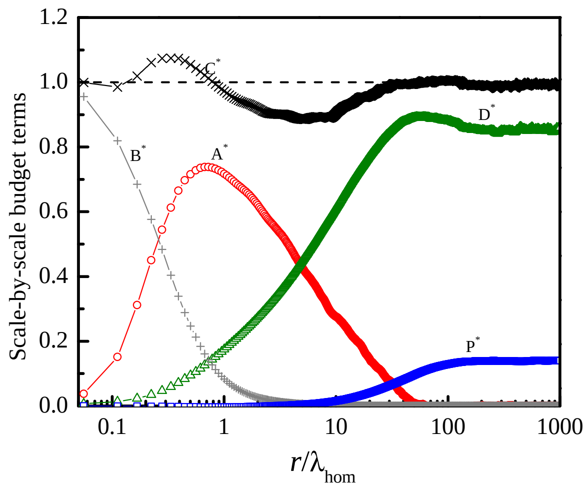

Figure 6: Terms in (19) at $x/D = 15$ along the centreline. Red (◯) is the advection term (A^*), gray $+$ is the diffusion term (B^*), green $\triangle$ is the decay term (D^*), blue $\square$ is the production term (P^*) and black $\times$ is the sum of all other terms ($C^* = A^* + B^* + D^* + P^*$).

following power-law of the form $\langle q^2 \rangle \propto (x - x_0)^m$ along the centreline. It was also suggested that the normalised third-order structure function can be estimated from the normalised second-order structure functions, power-law exponent, m, and decay rate constants of $\langle u^2 \rangle$ and $\langle v^2 \rangle$.

Experimental measurements were conducted at $Re_D = 50,000$ over the range $10 \leq x/D \leq 20$ along the centreline of a round jet to validate the theoretical analysis. It was found that a power-law decay region does exist over the present range of measurements for $\langle q^2 \rangle$ with $m = -1.83$. It was also shown that the distributions of $\langle (\delta q)^2 \rangle$, when normalised by $\langle q^2 \rangle$ and λ_{hom}, satisfied similarity to a close approximation over all range of scales. The calculated and measured distributions of the normalised third-order structure functions were found in better satisfactory in (16) than (25). Finally, the balance of all terms in (16), which was derived as a new self-similar equation for round jets, was investigated.

Acknowledgment

The authors acknowledge the financial support of the Natural Sciences and Engineering Research Council of Canada under their Discovery and RTI grant programmes.

REFERENCES

Antonia, R. A. & Burattini, P. 2006 Approach to the 4/5 law in homogeneous isotropic turbuelnce. *J. Fluid Mech.* **175**, 184.

Antonia, R. A., Smalley, R. J., Zhou, T., Anselmet, F. & Danaila, L. 2003 Similarity of energy structure functions in decaying homogeneous isotropic turbulence. *J. Fluid Mech.* **487**, 245–269.

Burattini, P. & Antonia, R. A. 2005 The effect of different X-wire calibration schemes on some turbulence statistics. *Exp. Fluids* **38**, 80–89.

Burattini, P., Antonia, R. A. & Danaila, L. 2005*a* Scale-by-scale energy budget on the axis of a turbulent round jet. *J. Turbul* **6**, 1–11.

Burattini, P., Antonia, R. A. & Danaila, L. 2005*b* Similarity in the far field of a turbulent round jet. *Phys. Fluids* **17**, 025101.

Danaila, L., Anselmet, F. & Antonia, R.A. 2002 An overview of the effect of large-scale inhomogeneities on small-scale turbulence. *Phys. Fluids* **14**, 2475.

Danaila, L., Anselmet, F., Zhou, T. & Antonia, R. A. 1999 A generalization of Yaglom's equation which accounts for the largescale forcing in heated decaying turbulence. *J. Fluid Mech.* **391**, 359 372.

Danaila, L., Antonia, R. A. & Burattini, P 2004 Progress in studying small-scale turbulence using exact two-point equations. *New J. Phys.* **6**, 1–28.

Fellouah, H., Ball, C. G. & Pollard, A. 2009 Reynolds number effects within the development region of a turbulent round free jet. *Int. J. Heat Mass Transfer* **52**, 39433954.

Ferdman, E., Otugen, M. V. & Kim, S. 2000 Effect of initial velocity profile on the development of the round jet. *J. Propul. Power* **4**, 676686.

George, W. K. 1992 The decay of homogeneous isotropic turbulence. *Phys. Fluids* **4** (7), 1492–1509.

Hearst, R. J., Buxton, O. R. H., Ganapathisubramani, B. & Lavoie, P. 2012 Experimental estimation of fluctuating velocity and scalar gradients in turbulence. *Exp. Fluids* **53**, 925–942.

Hussein, H. J., Capp, S. & George, W. K. 1994 Velocity measurements in a high-Reynolds number, momentum-conserving, axisymmetric, turbulent jet. *J. Fluid Mech.* **258**, 31–75.

Kolmogorov, A. N. 1941 The local structure of turbulence in incompressible viscous fluids for very large Reynolds numbers. *Dokl. Akad. Nauk SSSR* **30** (4), 301–305.

Lumley, J. L. 1965 Interpretation of time spectra measured in high-intensity shear flows. *Phys. Fluids* **8**, 1056.

Panchapakesan, N. R. & Lumley, J. L. 1993 Turbulence measurements in axisymmetric jets of air and helium. Part 1. Air jet. *J. Fluid Mech.* **246**, 197–223.

Sadeghi, H., Lavoie, P. & Pollard, A. 2014 The effect of Reynolds number on the scaling range along the centreline of a round turbulent jet. *J. Turbul.* **15**, 335349.

Sadeghi, H., Lavoie, P. & Pollard, A. 2015 Equilibrium similarity solution of the turbulent transport equation along the centreline of a round jet. *J. Fluid Mech.* **in press**.

Sadeghi, H. & Pollard, A. 2012 Effects of passive control rings positioned in the shear layer and potential core of a turbulent round jet. *Phys. Fluids* **24**, 115103.

Weisgraber, T. H. & Liepman, D. 1998 Turbulent structure during transition to self-similarity in a round jet. *Exp. Fluids* **24**, 210224.

Xu, G. & Antonia, R. A. 2002 Effect of different initial conditions on a turbulent round free jet. *Exp. Fluids* **33**, 677683.

Xu, M., Pollard, A., Mi, J., Secretain, F. & Sadeghi, H. 2013 Effects of Reynolds number on some properties of a turbulent jet from a long square pipe. *Phys. Fluids* **25**, 035102.